Efficient Hydroxyl Radical Production and Their Reactivity with Ethanol in the Presence of Photoexcited Semiconductors

Hiroyuki NODA,* Kazuo OIKAWA,† Hiroaki OHYA-NISHIGUCHI, and Hitoshi KAMADA
Institute for Life Support Technology, Yamagata Technopolis Foundation, 683 Kurumanomae, Numagi, Yamagata 990
† Yamagata Research Institute of Technology, 683 Kurumanomae, Numagi, Yamagata 990

(Received January 10, 1994)

ESR spin trapping technique has been applied to determine the quantum efficiency of the hydroxyl radical production from semiconductors such as anatase and rutile TiO_2, WO_3, and ZnO photoexcited with a 365 nm UV lamp in water and aqueous H_2O_2 solution. The quantum efficiency for anatase TiO_2, rutile TiO_2, and WO_3 in H_2O_2 solution was 3—4 times larger than that in water. Its maximum values, 4.6% in water and 14.8% in 1 mmol dm^{-3} H_2O_2 solution were obtained from anatase TiO_2. The reaction of the hydroxyl radical from photoexcited semiconductors with ethanol has been investigated in relation to the C-centered radical production in aqueous ethanol solution. The possible photocatalytic redox mechanisms are discussed concerning the reactions caused by photoinduced electron-hole pairs and produced radicals.

Many papers have been published on the photocatalysis on powdery semiconductors exhibiting strong oxidation and reduction abilities.[1—10] The hydroxyl radical, which is a strong oxidant, has been believed to play a major role in photocatalytic oxidation processes such as the oxidation of alcohol[11—14] and the production of phenol from benzene.[8] In our previous studies,[15,16] semiconductors such as anatase TiO_2, rutile TiO_2, and WO_3 were irradiated with photons of energy exceeding their respective band-gap energies in water and aqueous H_2O_2 solutions, and the production of the hydroxyl radical was confirmed by using the ESR spin trapping technique. It was also confirmed that the hydroxyl radical is produced from both the oxidation of water and the reduction of H_2O_2 by the photoinduced electron-hole pairs. The mechanism for such production was explained in terms of the energy band structures of the semiconductors, the redox potentials for the production of the hydroxyl radical, and the surface acidity and basicity of the semiconductors. In order to understand the photocatalytic oxidation processes in more detail, however, it is important to determine the quantum efficiency for the production of intermediates from photoexcited semiconductors.

A few papers[17] have been published on the quantum efficiency for the production of CO_2^- from photoexcited ZnO in water using the ESR spin trapping technique. Harbour and Hair,[17] for example, have measured the quantum efficiency for the production of CO_2^- induced by photoproduced holes and hydroxyl radicals. The quantum efficiency was determined as 4%. However, few studies have been reported on the quantum efficiency for the production of the hydroxyl radical, since the spin adducts are unstable during irradiation and the trapping efficiency is unknown. For the trapping experiments there was another practical difficulty of homogeneous mixing in the flat ESR cell.

In this study, such difficulties could be solved by using the high concentration solution of a high-purity spin trap reagent and by irradiating samples with the weak power of UV light. The quantum efficiency for the production of hydroxyl radicals from photoexcited semiconductors has been quantitatively determined by referring to the kinetic curves of the hydroxyl radical production obtained by the spin-trapping experiment. Furthermore, we have extended our study of the reaction of the produced hydroxyl radical to the reaction with alcohols, a typical example of photocatalytic reaction. In the following we will describe mainly the quantum efficiency of the hydroxyl radical production and the reactivity with ethanol.

Experimental

Materials. Powdery semiconductors such as anatase TiO_2 (99.9%), rutile TiO_2 (99.9%), WO_3 (99.5%), and ZnO (99.9%) were obtained from Wako Pure Chemical Industries, Ltd. As a spin trap reagent, 5,5-dimethyl-3,4-dihydro-2*H*-pyrole 1-oxide (DMPO) was obtained from Dojindo Laboratory. Aqueous hydrogen peroxide solutions (H_2O_2, 30%) and ethanol (special grade) were purchased from Wako Pure Chemical Industries, Ltd.

Apparatus. A flat quartz ESR cell was used in all of the experiments. Powdery semiconductors (1—2 mg) were dispersed in 1 ml of water. The powder suspensions (50 μl) were mixed with 21.8 μl of 9.2 mol dm^{-3} DMPO and 28.2 μl of water (or 1 mmol dm^{-3} H_2O_2 solutions or ethanol solution). High concentration of DMPO was necessary to trap effectively the produced hydroxyl radical and C-centered radical because production sites on the semiconductor surfaces are very close to one another and reaction rates for various compounds are very fast. The appropriate concentration of DMPO (2 mol dm^{-3}) for our experiments was decided by the results obtained from DMPO concentration dependence of the intensity of the hydroxyl radical and C-centered adducts. The saturation of the signal intensity was observed above 1 mmol dm^{-3}. Moreover, the same tangent at the starting point of irradiation was found between 0.5 and 2 mol dm^{-3} DMPO suspension. The concentration of H_2O_2 was selected so as to obtain the maximum intensity of the spin adduct, based on our previous study.[16] The suspension was fed into the ESR cell, which was inserted into the cavity of an ESR spectrometer (JEOL JES-RE3X).

The ESR measurements were conducted during irradiation of a 365 nm UV lamp Model EN-160L/J (Spectronics Co., USA) at room temperature. The quantum efficiency was determined by measuring the ratio of the number of trapped hydroxyl radicals to the number of photons per second estimated from the light intensity incident on the cell. The light intensity was measured by using a light power meter Spectronics Co. Model DRC-100X. The light intensity of the order of 30 $\mu W\,cm^{-2}$ was used throughout this experiment. Here we assumed that the incident light was completely absorbed by the powders, since no transmission of light from irradiation side to rear side of the flat ESR cell was detected. 4-Hydroxy-2,2,6,6-tetramethyl-1-piperidinyloxyl (TEMPOL, Aldrich Chem Co.) was used as a standard of radical concentration.

Results and Discussion

Kinetics of the Hydroxyl Radical Production. The ESR spectrum of the DMPO spin adducts from irradiated anatase TiO_2 containing 1 $mmol\,dm^{-3}$ H_2O_2 is shown in Fig. 1 as an example of the spectra measured. This spectrum could easily be assigned to the hydroxyl radical and hydroperoxyl (or superoxide ion) radical adducts in view of their hyperfine splitting constants. From these the stick diagrams of the spectra are obtained, as is also shown in the lower part of the figure.[18] By fixing the field at the position of the far-left signal of the hydroxyl radical adduct in Fig. 1, the time dependence of the radical concentration was traced in order to investigate the reaction behavior of the spin adduct.

The kinetic curves of the hydroxyl radical production from photoexcited semiconductors in water are shown in Fig. 2. The curves from anatase TiO_2, rutile TiO_2, and ZnO showed intensity maxima with time, which were in line with the results of Harbour and Hair[17] and Cresa et al.[19] The signal intensity leveled off when irradiation was stopped. The appearance of such maxima is probably due to competition between photoinduced production and extinction (reduction and oxidation) of the radical adduct catalyzed by the photoexcited semiconductors in accordance with the decrease in the concentration of oxygen. A peculiar behavior was observed for WO_3. The kinetic curve for WO_3 showed a monotonous increase with time. This may be related to the occurrence of the reduction of WO_3 itself (E=−0.45 V vs. NHE, pH=7), which means no reduction of spin adduct, with the decrease in the concentration of oxygen.

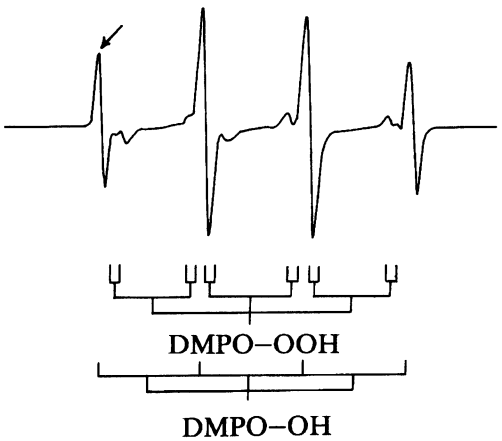

Fig. 1. ESR spectrum of the DMPO spin adducts obtained by 60-s irradiation of anatase TiO_2 suspensions in 1 $mmol\,dm^{-3}$ H_2O_2.

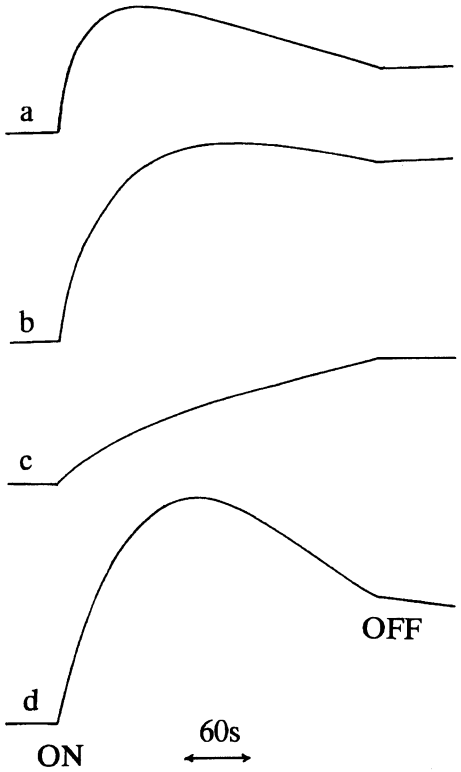

Fig. 2. Time profiles of the ESR signal intensity of the DMPO-OH during irradiation in water. a: anatase, b: rutile, c: WO_3, d: ZnO, receiver gain: ×100 (anatase, ZnO), ×200 (rutile and WO_3).

The kinetic curves for 1 $mmol\,dm^{-3}$ H_2O_2 solutions are shown in Fig. 3. For anatase TiO_2, rutile TiO_2, and WO_3, similar time courses but higher intensities of the adduct were observed in comparison with the case in water. The high intensities suggest that both the oxidation of water and the reduction of H_2O_2 occurred. This is probably because the reduction potential of H_2O_2 lies far enough below the conduction band edges of the semiconductors, as has already been discussed in detail.[15,16] For ZnO, however, the addition of H_2O_2 did not induce any effect. Similar intensity of the adduct and a similar kinetic curve with to those in water were observed, which means that no reduction of H_2O_2 by electrons had occurred. This result may have arisen from the difference of the adsorption of H_2O_2 on the ZnO surface having a basic property[16] or the occurrence for the oxidation of H_2O_2 by a hole with the oxidation of water. Moreover, this phenomenon is sim-

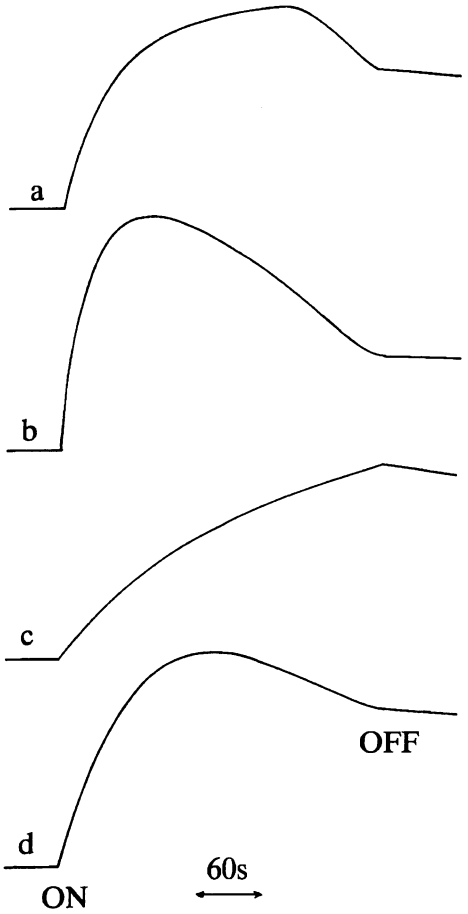

Fig. 3. Time profiles of the ESR signal intensity of the DMPO-OH during irradiation in 1 mmol dm^{-3} H_2O_2 solutions. a: anatase, b: rutile, c: WO_3, d: ZnO, receiver gain: ×25 (anatase), ×50 (rutile and WO_3), ×100 (ZnO).

ilar to the result of Harbour and Hair[20] that H_2O_2 is easily produced by irradiated ZnO under aerated conditions and accumulated in its suspensions. It is noted here that the accumulation of H_2O_2 does not cause any reduction of H_2O_2.

Determination of the Quantum Efficiency. The method for determination of the quantum efficiency is now described. In order to determine the quantum efficiency, it is necessary to estimate hydroxyl radical number or spin adduct concentration. For such purposes, double integration of the differential ESR spectrum measured is usually used, but in our case this method could not be applied because the spin adduct formed was decomposed gradually, as shown in Figs. 2 and 3. Alternatively, the number of hydroxyl radicals (n) was determined by the tangent of the kinetic curve at the starting point of irradiation described by the equation:

$$n = k \cdot H/t, \quad (1)$$

where k is a constant determined by referring to the intensity for the standard radical concentration, H is the signal height on the spectrum chart at a time t, and t is the time in seconds, all defined as shown in Fig. 4. The value k is determined by the method described in the following. The number of the radicals in the irradiation area (4.2×20 mm^2) was calibrated based both on the distribution of the ESR sensitivity at some position in the cell using TEMPOL impregnated filter paper (about 5 mmϕ), as shown in Fig. 5 and on the effective volume of the irradiation area in the cell (24 μl). Seventy percent of the total signal intensity was filled at the irradiation area. The difference of the line widths between DMPO-OH and TEMPOL was taken into accounts when estimating the number of the spin adducts by this equation:

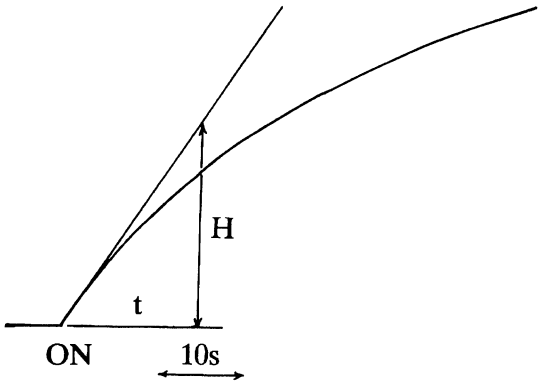

Fig. 4. Time profile of the ESR signal intensity of the DMPO-OH during irradiation.

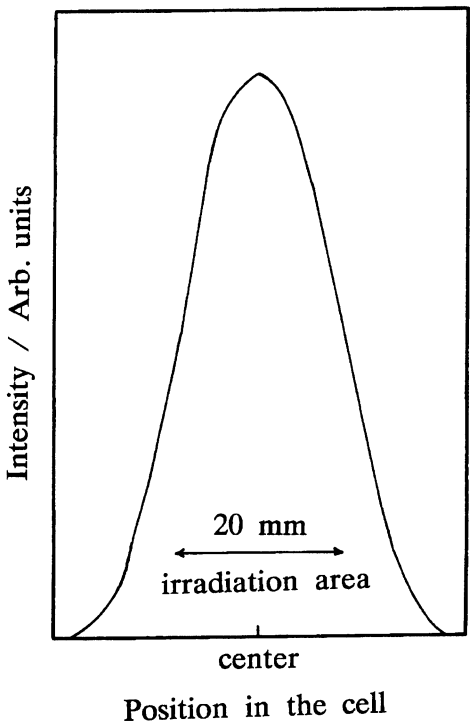

Fig. 5. Distribution of ESR sensitivity at some position in the cell using TEMPOL impregnated filter paper (about 5 mmϕ).

$$S_{\mathrm{TEMPOL}}(S_{\mathrm{DMPO-OH}}) = C \cdot h \cdot (\Delta H_{\mathrm{pp}})^2 \cdot N, \quad (2)$$

where S_{TEMPOL} and $S_{\mathrm{DMPO-OH}}$ are the values of the double integration of the differential ESR spectrum of TEMPOL and DMPO-OH, respectively, C is the constant for the spectrum pattern: Lorentzian or Gaussian, h is the signal height of the differential ESR spectrum, ΔH_{pp} is the peak-to-peak width of the differential ESR spectrum, and N is the number of hyperfine splittings. The values S are calculated by regarding each line shape as Lorentzian. The value k was calculated by using the above values. The number of incident photons was estimated from the light power.

The quantum efficiency values thus estimated for the production of the hydroxyl radicals are listed in Table 1. Here the quantum efficiency for the direct decomposition of H_2O_2 by photolysis was determined as 0.03% for the irradiation of aqueous H_2O_2 solutions. The values in water are in the order, anatase TiO_2 > rutile TiO_2 > ZnO > WO_3. On the other hand, in 1 mmol dm^{-3} H_2O_2 solutions, the values are 3 to 4 times larger than those in pure water, with the order of anatase TiO_2 > rutile TiO_2 > WO_3. Contrarily, the values for the combination of ZnO and H_2O_2 are appreciably lower than that in water. The values for anatase TiO_2, rutile TiO_2, and WO_3 are appreciably larger than those from the decomposition of H_2O_2 in the absence of semiconductors (0.03%). Furthermore, the values of TiO_2 are of the same order as or high compared with the values for the production of H_2 using TiO_2.[21]

Maximum values of the quantum efficiency of 4.6% in water and 14.8% in aqueous H_2O_2 solutions were obtained from anatase TiO_2. The values for anatase TiO_2, rutile TiO_2, and WO_3 in 1 mmol dm^{-3} H_2O_2 solutions were 3—4 times larger than those in water. These results suggest that the separation efficiency of an electron-hole pair improves with addition of H_2O_2 as a reductant. The same behavior has been reported in the oxygen-saturated case.[19]

Reactions in Aqueous Ethanol Solutions. We have carried out experiments examining the reaction between the hydroxyl radical and ethanol, in order to clarify the photocatalytic oxidation process of ethanol. The ESR spectra of the DMPO spin adducts from irradiated anatase TiO_2 in water and in 20% of ethanol solution are shown in Fig. 6 a and b. In ethanol solutions, the C-centered adduct and hydroxyl radical

Table 1. The Quantum Efficiency Values (Φ)

Semiconductor	Φ[a]/%	
	Water	1 mmol dm^{-3} H_2O_2
Anatase	4.6	14.8
Rutile	3.2	13.1
WO_3	0.5	2.0
ZnO	2.4	—

a) The average values of three times measurements.

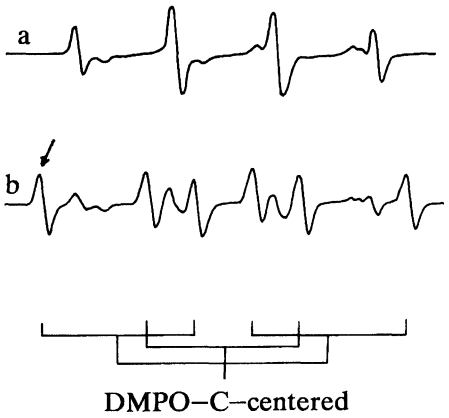

Fig. 6. ESR spectra of the DMPO spin adducts obtained by 20-s irradiation of anatase TiO_2 suspensions in water and aqueous ethanol solutions. a: in water, b: in 20% ethanol.

adduct were observed with a trace amount of the superoxide ion adduct. Similar behavior was observed from anatase TiO_2 in aqueous H_2O_2 solutions and from the other semiconductors in water and H_2O_2 solutions. The amount of produced adducts could be relatively estimated by comparing the intensities of the far-left signals of DMPO-OH (1 : 2 : 2 : 1) and DMPO-C-centered (1 : 1 : 1 : 1 : 1 : 1) with each other and by comparing their time dependences, because the two linewidths are equal. In Fig. 6, the intensity of the C-centered adduct in 20% ethanol solutions was larger than that of the hydroxyl radical. This result make it seem as if the oxidation of ethanol by hole had occurred along with that by the hydroxyl radical. However, this intensity ratio may also be related to the stability of the spin adducts themselves. Therefore, this ratio will be discussed by using both kinetic curves in the following section.

The time dependence of the C-centered radical adduct production was also traced by fixing the field at the position of the far-left signal of the adduct shown in Fig. 6. The kinetic curves of the hydroxyl radical and the C-centered radical adducts from anatase TiO_2 in water and in 20% ethanol solution are compared in Fig. 7. A little difference was observed between these time profiles. This result is believed to relate to both the differences of the stabilities of the spin adducts and of the concentrations of electron acceptor (e.g. dissolved oxygen[19]). The tangent of the kinetic curve for the hydroxyl radical production at the starting point of irradiation was more steep than that for the C-centered radical production. This indicates that the quantity of hydroxyl radical production is higher than that of C-centered radical production.

The ethanol concentration dependence for the intensities of the DMPO spin adducts, which are obtained by the values of the tangent at the starting point of irradiation, is shown in Fig. 8. The increase of the ethanol concentration led to an increase in the intensity of

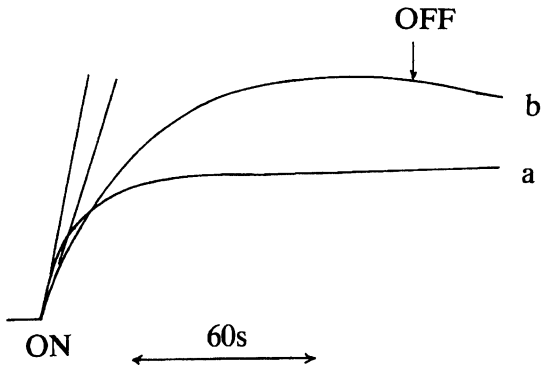

Fig. 7. Time profiles of the ESR signal intensity of the DMPO spin adducts during irradiation in water and aqueous ethanol solutions. a: in water, b: in 20% ethanol.

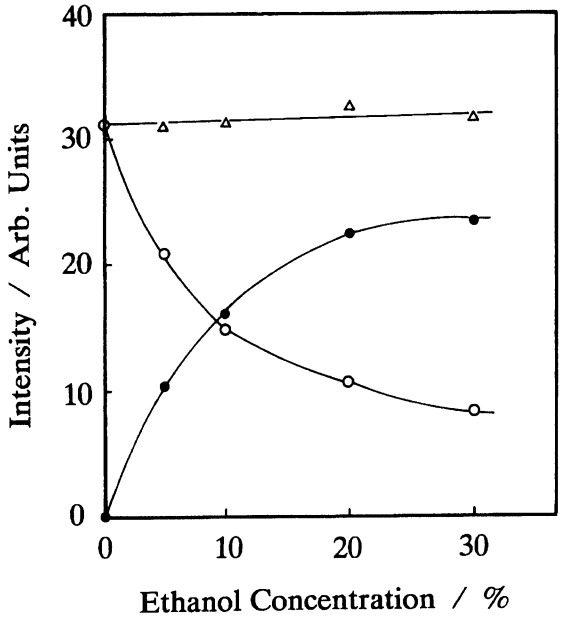

Fig. 8. Ethanol concentration dependence of the DMPO spin adducts. open circle: DMPO-OH, closed circle: DMPO-C-centered, open triangle: DMPO-OH+DMPO-C-centered.

the C-centered adduct and to a concomitant decrease in the intensity of the hydroxyl radical adduct. The total quantity of the spin adducts production slightly increases with the increase of the ethanol concentration. This means that the oxidation of ethanol by the hydroxyl radicals occurs mainly and that due to holes is only a little, because the rate of the reaction between the hydroxyl radical and ethanol (or DMPO) is very fast as described above and almost all of the produced hydroxyl radical react with ethanol or DMPO, depending on their concentration. This consideration is also supported by the reasoning that the quantity of the hydroxyl radical production in aqueous ethanol solutions and that in water are nearly equal under these conditions, because the concentration of water is one order larger than that of ethanol. Strictly speaking, not only the concentration of water and ethanol but also the surface hydrogen bond may influence in the photocatalytic oxidation of ethanol. The analysis of these results suggests that the C-centered adducts is mainly produced through the reaction between the hydroxyl radical and ethanol under these conditions. The increase in the concentration of ethanol above 50% led to a decrease in that of the C-centered adduct and caused a broadening in the ESR signal. Therefore, we do not discuss the photocatalytic oxidation process under the high concentration of ethanol.

Mechanism of Photocatalytic Redox Reactions. From the analysis of above results, the photocatalytic reactions in aerated aqueous ethanol solutions can be described as follows:

$$\text{Semiconductor} + h\nu \rightarrow e^- + h^+, \quad (3)$$

$$O_2 + e^- \rightarrow O_2^-, \quad (4)$$

$$H_2O + h^+ \rightarrow \cdot OH + H^+, \quad (5)$$

$$H_2O_2 + H^+ + e^- \rightarrow \cdot OH + H_2O, \quad (6)$$

$$\text{Semiconductor} + e^- \rightarrow \text{selfreduction}, \quad (7)$$

$$\text{Semiconductor} + h^+ \rightarrow \text{selfoxidation}, \quad (8)$$

$$CH_3CH_2OH + \cdot OH(h^+) \rightarrow \cdot CH(CH_3)OH + H_2O(H^+), \quad (9)$$

$$\cdot CH(CH_3)OH + \cdot OH(h^+) \rightarrow CH_3CHO + H_2O(H^+). \quad (10)$$

The photoexcited semiconductor produces an electron-hole pair [reaction (3)]. Dissolved oxygen is reduced by photoproduced electrons [reaction (4)] and water is oxidized by photoproduced holes [reaction (5)]. In the presence of H_2O_2, reaction (6) is caused by photoproduced electrons, except for ZnO. The selfreduction [reaction (7)] occurs on a semiconductor having high reduction potential, such as WO_3.[22] The selfoxidation [reaction (8)] occurs on a semiconductor having low oxidation potential such as ZnO.[23] And reactions (9) and (10) are mainly caused by the hydroxyl radical in the presence of ethanol (<50%). Moreover, the following reactions are expected to occur after an addition of DMPO as a spin trap reagent in this system.

$$O_2^- + \text{DMPO} \rightarrow \text{DMPO} - OO^- \quad (11)$$

$$\cdot OH + \text{DMPO} \rightarrow \text{DMPO} - OH \quad (12)$$

$$\cdot CH(CH_3)OH + \text{DMPO} \rightarrow \text{DMPO} - \text{C} - \text{centered} \quad (13)$$

The produced radicals are trapped by DMPO depending on the reaction rates between DMPO and

radicals.[24] The reaction rates of reactions (9) and (12) are of the same order[25] and that of reaction (13) is one order smaller.[26] Therefore, the concentration of DMPO and ethanol are important for examining the reaction between the hydroxyl radical and ethanol. In fact, DMPO-OH spin adduct decreased in 0.1 mol dm^{-3} DMPO solution and no DMPO-OH adduct was observed in 0.01 mol dm^{-3} DMPO solution. The following reactions having large reaction rates[27,28] must be considered because the production site of the hydroxyl radical and the superoxide ion (or the hydroxyl radical) is very close.

$$O_2^- + \cdot OH + H^+ \rightarrow H_2O + O_2 \quad (14)$$

$$\cdot OH + \cdot OH \rightarrow H_2O_2 \quad (15)$$

Reactions (14) and (15) should occur in photoexcited semiconductor systems. However, the concentration of produced radicals is much lower than that of DMPO and ethanol. Moreover, the production of the hydroxyl radical which originated from three electron reduction of oxygen ($O_2 \rightarrow O_2^- \rightarrow H_2O_2 \rightarrow \cdot OH$) was confirmed by the experiments in water under the addition of both SOD and catalase [reactions (16) and (6)]. The addition of SOD promotes reaction (16) and the addition of catalase promotes reaction (17). The decreased hydroxyl radical adduct was observed under the addition of both SOD and catalase. If the hydroxyl radical was produced through the reduction of H_2O_2, the decreased hydroxyl radical adduct should be observed under the addition of catalase. The Harber–Weiss reaction [reaction (18)] was negated, because no change in the signal intensity was observed under the addition of SOD. If reaciton (18) is related to the hydroxyl radical production, a change in the signal intensity would be observed.

$$O_2^- + 2H^+ + e^- \rightarrow H_2O_2 \quad (16)$$

$$2H_2O_2 \rightarrow 2H_2O + O_2 \quad (17)$$

$$O_2^- + H_2O_2 + H^+ \rightarrow \cdot OH + H_2O + O_2 \quad (18)$$

Therefore, the effect of reactions (14) and (15) in our experiments is believed to be small. The photocatalytic extinction of DMPO-OH adduct with an increase of the irradiation times is considered to be due to following two reactions:

$$\text{DMPO} - \text{OH} + \cdot OH \rightarrow \text{oxidative product (ESR silent)}, \quad (19)$$

$$\text{DMPO} - \text{OH} + e^- + H^+ \rightarrow \text{reduced product (ESR silent)}. \quad (20)$$

In TiO_2, WO_3, and ZnO suspensions, reaction (19) occurs with both an increase in the concentration of produced DMPO-OH and a decrease in the concentration of DMPO around the semiconductor surface. In TiO_2 and ZnO suspensions, reaction (20) also occurs with a decrease in the electron acceptors such as oxygen. In WO_3 suspension, reaction (20) does not occur due to the occurrence of selfreduction.

In summary, we have demonstrated that the quantum efficiency of the hydroxyl radical production from photoexcited semiconductors can be determined by using the ESR spin tapping technique in water and in aqueous H_2O_2 solution. The quantum efficiency of the hydroxyl radical production determined in this study is sufficiently high, which implies that the hydroxyl radical plays a major role in photocatalytic oxidation process. The experimental results in aqueous ethanol solutions indicate that the C-centered radical is mainly produced from the oxidation of ethanol by the hydroxyl radical. The mechanisms of the photocatalytic redox reactions caused by photoproduced electron-hole pairs can be explained by using all of the reactions considered.

References

1) M. Grätzel, *Ber. Bunsen-Ges. Phys. Chem.*, **84**, 981 (1980).
2) T. Kawai and T. Sakata, *Nature*, **286**, 474 (1980).
3) K. Kalyanasudaram, E. Borgarello, and M. Grätzel, *Helv. Chim. Acta.*, **64**, 362 (1981).
4) B. Anrian-Blajeni, M. Halmann, and J. Manasen, *Sol. Energy*, **25**, 165 (1980).
5) G. N. Schrauzer and T. D. Guth, *J. Am. Chem. Soc.*, **99**, 7189 (1877).
6) S. Sato and J. M. White, *Chem. Phys. Lett.*, **70**, 131 (1989).
7) T. Kanno, T. Oguchi, H. Sakuragi, and K. Tokumaru, *Tetrahedron Lett.*, **21**, 467 (1980).
8) I. Izumi, W. W. Dunn, K. O. Wilbourn, F. -R. F. Fan, and A. J. Bard, *J. Phys. Chem.*, **84**, 3207 (1980).
9) H. Reiche and A. J. Bard, *J. Am. Chem. Soc.*, **101**, 3127 (1979).
10) K. Hashimoto, T. Kawai, and T. Sakata, *J. Phys. Chem.*, **88**, 4083 (1984).
11) T. Kawai and T. Sakata, *J. Chem. Soc., Chem. Commun.*, **1980**, 694.
12) T. Sakata and T. Kawai, *Chem. Phys. Lett.*, **80**, 341 (1981).
13) S. Nishimoto, B. Ohtani, A. Sakamoto, and T. Kagiya, *Nippon Kagaku Kaishi*, **1984**, 246.
14) H. Noda, K. Oikawa, T. Ogata, K. Matsuki, and H. Kamada, *Nippon Kagaku Kaishi*, **1986**, 1084.
15) H. Noda, K. Oikawa, and H. Kamada, *Bull. Chem. Soc. Jpn.*, **65**, 2505 (1992).
16) H. Noda, K. Oikawa, and H. Kamada, *Bull. Chem. Soc. Jpn.*, **66**, 455 (1993).
17) For example: J. R. Harbour and M. L. Hair, *J. Phys. Chem.*, **83**, 652 (1979).
18) G. R. Buettner, *Free Rad. Biol. Med.*, **3**, 259 (1987).
19) E. M. Cresa, L. Burlamacchi, and M. Viska, *J. Mater. Sci.*, **18**, 289 (1983).
20) J. R. Harbour and M. L. Hair, *Adv. Colloid Interface Sci.*, **24**, 103 (1986).

21) T. Kawai and T. Sakata, *J. Chem. Soc., Chem. Commun.*, **1980**, 694.
22) M. Fujii, T. Kawai, H. Nakamatsu, and S. Kawai, *J. Chem. Soc., Chem. Commun.*, **1983**, 1428.
23) H. Gerischer, *J. Electrochem. Soc.*, **113**, 1174 (1966).
24) E. Finkelstein, G. M. Rosen, and E. J. Rauckman, *J. Am. Chem. Soc.*, **102**, 4994 (1980).
25) B. S. Wolfenden and R. L. Willson, *J. Chem. Soc., Perkin Trans. 2*, **1982**, 805.
26) H. Noda, unpublished data.
27) K. Sehested, O. L. Rasmussen, and H. Fricke, *J. Phys. Chem.*, **72**, 626 (1968).
28) R. Pagsberg, H. Christensen, J. Rabani, G. Nilsson, J. Fenger, and S. O. Nielsen, *J. Phys. Chem.*, **73**, 1029 (1969).